RESEARCH ARTICLE

Genome-Wide Methylation Analysis in Vestibular Schwannomas Shows Putative Mechanisms of Gene Expression Modulation and Global Hypomethylation at the HOX Gene Cluster

Miguel Torres-Martín,[1]* Luis Lassaletta,[2] Jose M de Campos,[3] Alberto Isla,[4] Giovanny R. Pinto,[5] Rommel R. Burbano,[6] Bárbara Melendez,[7] Javier S. Castresana,[8] and Juan A. Rey[1]

[1] Molecular Neuro-oncogenetics Laboratory, Research Unit, Hospital Universitario La Paz, IdiPAZ, Madrid, Spain
[2]Department of Otolaryngology, Hospital Universitario La Paz, IdiPAZ, Madrid, Spain
[3]Neurosurgery Department, Fundacion Jimenez Diaz, Madrid, Spain
[4]Neurosurgery Department, Hospital Universitario La Paz, IdiPAZ, Madrid, Spain
[5]Genetics and Molecular Biology Laboratory, Federal University of Piau, Parnaiba, Brazil
[6]Human Cytogenetics Laboratory, Institute of Biological Sciences, Federal University of Para, Belem, Brazil
[7]Molecular Pathology Research Unit, Virgen de la Salud Hospital, Toledo, Spain
[8]Department of Biochemistry and Genetics, University of Navarra School of Sciences, Pamplona, Spain

Schwannomas are tumors that develop from Schwann cells in the peripheral nerves and commonly arise from the vestibular nerve. Vestibular schwannomas can present unilaterally and sporadically or bilaterally when the tumor is associated with neurofibromatosis Type 2 (NF2) syndrome. The molecular hallmark of the disease is biallelic inactivation of the *NF2* gene. The epigenetic signature of schwannomas remains poorly understood and is mostly limited to DNA methylation of the *NF2* gene, whose altered expression due to epigenetic factors in this tumor is controversial. In this study, we tested the genome-wide DNA methylation pattern of schwannomas to shed light on this epigenetic alteration in these particular tumors. The methodology used includes Infinium Human Methylation 450K BeadChip microarrays in a series of 36 vestibular schwannomas, 4 nonvestibular schwannomas, and 5 healthy nerves. Our results show a trend toward hypomethylation in schwannomas. Furthermore, homeobox (HOX) genes, located at four clusters in the genome, displayed hypomethylation in several CpG sites in the vestibular schwannomas but not in the nonvestibular schwannomas. Several microRNA (miRNA) and protein-coding genes were also found to be hypomethylated at promoter regions and were confirmed as upregulated by expression analysis; including miRNA-21, Met Proto-Oncogene (*MET*), and *PMEPA1*. We also detected methylation patterns that might be involved in alternative transcripts of several genes such as *NRXN1* or *MBP*, which would increase the complexity of the methylation and expression patterns. Overall, our results show specific epigenetic signatures in several coding genes and miRNAs that could potentially be used as therapeutic targets.

INTRODUCTION

Schwannomas are low-grade tumors that arise from the Schwann cells of peripheral nerves. Although these tumors can originate from numerous locations, they usually develop from the vestibulocochlear nerve, accounting for up to 10% of intracranial tumors. Vestibular schwannomas can be sporadic and unilateral or bilateral when they are associated with the genetic disorder known as neurofibromatosis Type 2 (NF2) syndrome. Current treatment options for schwannomas include "wait and scan," surgery and radiosurgery. Although recurrence is generally not expected, the consequences of treatment for patients can be devastating, especially for patients who have several tumors, such as NF2 patients. The most common molecular disorder of vestibular schwannomas is the mutation of the *NF2* tumor-suppressor gene and loss of heterozygosity (LOH) in the locus of this gene at chromosome arm 22q,

Additional Supporting Information may be found in the online version of this article.

Supported by: Fondo de Investigaciones Sanitarias, Ministerio de Ciencia e Innovación, Spain, Grant numbers: PI13/00055 (J.A.R.) and PI13/00800 (B.M.).

*Correspondence to: Miguel Torres-Martín. E-mail: migtorres.martin@gmail.com

Received 10 June 2014; Revised 9 November 2014; Accepted 25 November 2014

DOI 10.1002/gcc.22232

Published online 00 Month 2014 in Wiley Online Library (wileyonlinelibrary.com).

which at the cytogenetic level was observed as monosomy of chromosome 22 (Rey et al., 1987; Bello et al., 1993). *NF2* encodes for Merlin, a FERM domain protein that has two main isoforms and a wide variety of functions. Tumor mechanisms via the loss of Merlin function occur in the cytosol (via internalization of tyrosine kinase receptors, the hippo pathway or angiomotin; Yi et al., 2011) and the nucleus, suppressing tumorigenesis by inhibiting the ubiquitin ligase $CRL4^{DCAF1}$ (Li et al., 2010). Other molecular alterations include ErbB2-ErbB3/Nrg1 constitutional activation (Doherty et al., 2008), caveolin-1 downregulation (Aarhus et al., 2010), and *MET* and osteopontin upregulation, which has been suggested as an alternative to Merlin degradation in schwannomas (Torres-Martin et al., 2013a, 2013b). It has also been proposed that a Yes-associated protein 1 (*YAP*)-driven signaling network induces tumor proliferation (Boin et al., 2014). Several clinical trials on treating schwannomas in NF2 patients have been conducted in recent years, a number of which have had promising outcomes (Plotkin et al., 2009), while others have shown no patient improvement (Plotkin et al., 2010; Karajannis et al., 2014).

Among epigenetic mechanisms, cytosine methylation at CpG dinucleotides is probably the most widely studied. The CpG sites are usually clustered within the DNA in enriched zones known as CpG islands, flanked by less enriched shores and then by shelves. Methylation has been studied in gene promoter at transcriptional start site (TSS) and 5′-UTR regions, normally in connection with mRNA transcriptional repression. Nevertheless, current research is increasing attention on the lesser-known mechanisms of action of methylation within gene bodies and 3′-UTR regions. Recent experiments have shown that intragenic DNA methylation might be related to the regulation of alternative promoters (Maunakea et al., 2010) or to controlling transcriptional noise (Huh et al., 2013). The methylation processes for diseases such as cancer have been widely reported (Portela and Esteller 2010). Tumor-suppressor gene silencing and oncogene hypomethylation are well-known mechanisms of tumor development. The individual patient response to treatment can be predicted, such as the glioma response to alkylating agents based on *MGMT* methylation status (Esteller et al., 2000). MicroRNA (miRNA) also present aberrant epigenetic processes, in the same manner as protein-coding genes (Lopez-Serra and Esteller 2012). DNA methylation also participates in embryogenesis and tissue development, with homeobox (HOX) cluster genes playing a pivotal role in this process.

In schwannomas, the aberrant methylation of genes (including *THBS1*, *MGMT*, *TP73*, and *TIMP3*) has been identified by methylation-specific PCR (Gonzalez-Gomez et al., 2003; Bello et al., 2007). *NF2* methylation does not seem to be a mechanism of Merlin loss in schwannomas (Koutsimpelas et al., 2012; Lee et al., 2012), although specific CpG sites might be involved (Kino et al., 2001). Thus, the epigenetic landscape of schwannomas remains poorly described and understood. Current wide epigenetic genomic profiling techniques include next generation sequencing and microarray technology. Using these techniques, numerous prognostic factors have been identified, including the CpG island methylator phenotype in various tumors such as oligodendrogliomas (Mur et al., 2013) and ependymomas (Mack et al., 2014). Using the Illumina 450k Infinium BeadChip kit, we tested 485,000 individual CpG sites to find aberrant methylation in 36 vestibular and 4 nonvestibular schwannomas. Our aim was to detect aberrant methylation along tumors, differential methylation of CpG sites based on clinical characteristics and ultimately to find potential therapeutic targets. These findings were correlated with whole genome expression data from our previous analysis of the same cases, to determine whether there was any relationship between distinct epigenetic changes and gene expression variations.

MATERIALS AND METHODS

Samples and DNA/RNA Preparation

The study was performed on 40 tumors from 39 patients (16 men and 23 women) who underwent surgery in our institution. The local ethics review board of University Hospital La Paz approved the study protocol according to the principles of the Declaration of Helsinki. All patients received detailed information on the study and provided their written informed consent prior to their inclusion. The study population included 36 cases of vestibular schwannoma, six of which were related to NF2 syndrome. Four sporadic nonvestibular schwannomas were also added to the study (three spinal and one cervical). For control purposes, five healthy nerves with exclusive axonal content were used. DNA was isolated using the Wizard Genomic DNA purification kit (Promega). DNA

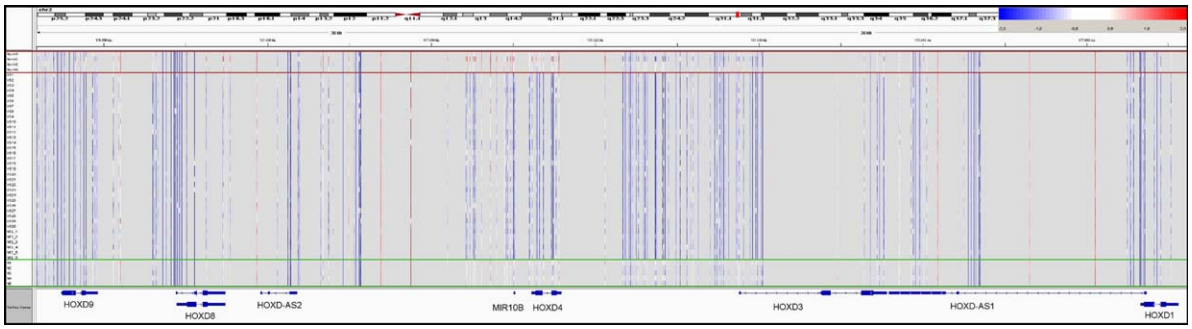

Figure 1. HOXD gene cluster at chromosome 2 shows hypomethylation processes. *M*-value graphical representation. Blue intensity reflects unmethylation, while red shows methylation. Control nerves are bounded by a green box, while nonvestibular schwannomas are above (red box). Vestibular samples are not highlighted. The miRNA-10b, present at the cluster, also had the same alteration.

from the corresponding patients' peripheral blood was also extracted. RNA from the four nonvestibular schwannomas was isolated using the RNeasy® Mini Kit (Qiagen).

Methylation Microarray Protocol

For the methylation analysis, 1 μg of DNA from the 40 tumors and 5 healthy nerves was treated with bisulfite using the EZ DNA methylation Kit (Zymo Research), according to the manufacturer's instructions. The converted DNA was then hybridized on the Infinium Human Methylation 450K BeadChip (Illumina), which examines 485,577 CpG sites across the whole genome. Arrays were processed at CEGEN, and the data can be accessed at the gene expression omnibus (GEO) database GSE56596.

Infinium Human Methylation 450K BeadChip Analysis

The analysis was performed using R statistical software. To import iDAT files into the R environment for processing, the lumi package was used (Du et al., 2008). After importing the iDAT files, we obtained a MethyLumiM class object. First, a background correction was performed with the bgAdjust method, and color bias was adjusted by the quantile method. Color bias adjustment was performed because the differences between the red and green channels were very pronounced (Supporting Information Fig. 1). Normalization was performed using simple scaling normalization. *M*-values were used instead of *B*-values due to the severe heteroscedasticity of the data when they were not in the middle of the methylation range (Du et al., 2010); *M*-values were, therefore, more statistically valid. After processing the data, the methyAnalysis package was used for data visualization in the integrative genomics viewer (Robinson et al., 2011; Thorvaldsdóttir et al., 2013). This task was performed by converting the MethyLumiM class into the MethyGenoSet class. Next, the *export.methyGenoSet* function was used to create a .cgt file. *M*-values were exported to a text file, and the data were then analyzed with an Illumina Methylation Analyzer (IMA) package (Wang et al., 2012). The necessary *P* values were obtained from GenomeStudio. With IMA functions, probes from X and Y chromosomes were removed due to the bias between male and female. In addition, low-quality CpG sites (P value > 0.05 in 75% of the samples) were filtered, as were probes containing SNPs. Methylation index calculations were performed at gene-based (TSS, 5′-UTR, first exon, Gene Body, and 3′-UTR region) and CpG location-based regions (CpG island, shores, and shelves). This process was performed using the *regionswrapper* command, which is explained by Wang et al. (2012). The specific methylation between groups for each CpG was analyzed using Student's *t*-test. Differential methylation among the groups was established at the Bonferroni-adjusted *P* value <0.05 and an *M*-value cutoff of 1. This value is within the range recommended by Du et al., (2010). Four groups of samples were created: sporadic vestibular schwannomas, NF2-related vestibular schwannomas, nonvestibular schwannomas, and control nerves. Since both vestibular groups were homogeneous, we combined those two groups for comparison against healthy tissue and nonvestibular schwannomas. Additionally, vestibular samples were classified by clinical group. An enrichment analysis of hypermethylated and hypomethylated genes was performed using DAVID (Huang et al., 2009) with a single CpG list, removing duplicates and CpG sites

with no associated name. In both lists, the total number of genes was below the limit supported by DAVID.

Expression Microarrays

To investigate whether the methylation pattern had an impact on gene expression, we used our previously published and available gene expression microarray data on the same series of vestibular schwannomas (Torres-Martin et al., 2013a, 2013b) and miRNAs (Torres-Martin et al., 2013a, 2013b) to compare with the methylation data. We defined a gene or miRNA as deregulated when we detected at least a 2-fold change in expression and a $P < 0.05$ cutoff by Student's *t*-test. For the *regionswrapper* analysis from the IMA package, the genes that met those criteria were selected. MultiExperiment Viewer (MeV) software (Saeed et al., 2003, 2006) was used for the expression array analysis.

The four nonvestibular schwannomas that were not included in our previous analysis were tested with microarrays. Briefly, Human Gene 1.0 ST arrays were hybridized as previously described (Torres-Martin et al., 2013a, 2013b). Normalization and summarization were performed using the RMA (robust multichip average) algorithm and were batch corrected with the other vestibular tumors using ComBat (Johnson et al., 2007). An exon-level analysis, which allowed us to test several isoforms of a given gene, was used. All statistical analyses were performed using MeV. The principal component analysis (PCA) was performed by eigenvalue decomposition of the three principal components for three-dimensional classification of the samples. The data can be accessed at GEO database GSE56597.

Clinical Data

The tumor was on the left side in 50% of the cases. Tumor sizes were classified by the KOOS scale as Stage 1 (intracanalicular; one case), Stage 2 (in which the largest diameter in the cerebellopontine angle (CPA) is 15 mm; eight cases), Stage 3 (16–30 mm in the CPA; 17 cases) or Stage 4 (>30 mm in the CPA; six cases). The tumor appearance was homogeneous in 20 patients, heterogeneous in 8 and cystic in 4. The fundus of the internal auditory canal (IAC) was involved in 22 cases and not in 10 cases. All tumor tissues obtained during surgery were fixed in 10% formalin and embedded in paraffin. Staining with hematoxylin–eosin was performed for routine microscopic diagnosis. Antoni Type A regions consisted of interwoven bundles of long bipolar spindle cells, whereas Antoni Type B regions showed a loose myxoid background containing more stellate tumor cells. The percentage of the various tissue types (A, B, and mixed) in each tumor sample was assessed independently by two pathologists. The results were grouped into two types: Type A, >70% of the tumor composed of Type A tissue; and Type B, <70% of the tumor composed of Type A tissue. No clinical data were available from nonvestibular cases.

Mutational Screening of *NF2* and LOH of Chromosome Arm 22q Analysis

The *NF2* gene was mutation tested by PCR/dHPLC, as previously described (Torres-Martin et al., 2013a). In brief, mutational screening was performed using dHPLC following the manufacturer's instructions (Transgenomic WAVE® dHPLC Systems). Samples with varying patterns by dHPLC were sequenced bidirectionally (ABI 3100-Avant, Applied Biosystems), using the BigDye sequencing kit (Applied Biosystems), to determine the position and nature of the alterations. We also conducted an multiplex ligation-dependent probe amplification (MLPA) analysis with SALSA P044 (MRC-Holland), which is able to detect large gene deletions or amplifications. The LOH analysis was performed using five microsatellite markers at 22q11-q12.3.

RESULTS

An Overall View of Vestibular Schwannoma Methylation Patterns Shows a Trend Toward Hypomethylation

A total of 6553 CpG sites were hypermethylated in vestibular schwannomas at autosomes when they were compared with control nerves (corrected *P*-value and *M*-value differences of at least 1). Hypomethylation occurred in 8307 CpG sites, suggesting that this alteration was more common in the tumors. All CpG sites with differential methylation are presented in Supporting Information Table 1. Through chromosome shredding (Table 1), we observed that hypomethylation was more frequent in all autosomes except at chromosomes 16, 19, and 22, where hypermethylation involved more CpG sites. Chromosomes 2, 10, 12, and 21 had greater hypomethylation among its probes. Using genes as references for a given CpG, we

TABLE 1. Chromosome Methylation Pattern in Vestibular Schwannomas

Chromosome	Total probes	Hypermethylation (%)	Hypomethylation (%)
1	35994	654 (1.82)	838 (2.33)
2	26725	546 (2.04)	764 (2.86)
3	19584	344 (1.76)	476 (2.43)
4	15512	238 (1.53)	336 (2.17)
5	18750	372 (1.98)	449 (2.39)
6	26873	527 (1.96)	596 (2.22)
7	22626	376 (1.66)	543 (2.40)
8	15890	358 (2.25)	388 (2.44)
9	7596	119 (1.57)	152 (2.00)
10	18503	358 (1.93)	509 (2.75)
11	22226	401 (1.80)	537 (2.42)
12	18943	284 (1.50)	484 (2.56)
13	9310	243 (2.61)	283 (3.04)
14	11453	171 (1.49)	251 (2.19)
15	11740	200 (1.70)	291 (2.48)
16	16691	353 (2.11)	327 (1.96)
17	21548	459 (2.13)	505 (2.34)
18	4531	64 (1.41)	95 (2.10)
19	19721	236 (1.20)	218 (1.11)
20	7811	105 (1.34)	114 (1.46)
21	3168	60 (1.89)	89 (2.81)
22	6579	85 (1.29)	62 (0.94)

Hypermethylation and hypomethylation were calculated using the Bonferroni-adjusted *P*-value <.05 and an *M*-value cutoff of 1.

established six categories for each mRNA transcript (TSS1500, TSS200, 5′UTR, 1st exon, gene body, and 3′UTR). In all six regions, the hypomethylation was constant but was more frequent in the 3′UTR regions, followed by the 5′UTR and gene body regions (Table 2). The TSS regions and the first exon region were almost equal in the number of altered CpG sites. In terms of the location of a CpG site in an epigenetic context (in an island, shore or shelf), hypermethylation appeared more relevant on islands and slightly less so at the shores, while hypomethylation was greatly increased at island shelves and in open sea. By a significant margin, the open sea region had the most alterations in terms of total numbers. The north–south shores and shelves had similar levels in terms of the percentage of methylated and hypomethylated CpG sites. In relative numbers, the islands were less affected by epigenetic mechanisms.

TABLE 2. Probes Organized by Location of a Particular CpG Site

Region	CpG sites	Hypermethylation (%)	Hypomethylation (%)
TSS1500	63514	723 (1.14)	755 (1.19)
TSS200	45956	297 (0.65)	330 (0.72)
5′UTR	48878	606 (1.24)	935 (1.91)
First Exon	28955	207 (0.71)	232 (0.80)
Gene Body	131532	2948 (2.24)	3842 (2.92)
3′UTR	14438	294 (2.04)	508 (3.52)
Island	112398	788 (0.70)	665 (0.59)
N_Shore	47915	926 (1.93)	865 (1.81)
S_Shore	37332	651 (1.74)	656 (1.76)
N_Shelf	18342	409 (2.23)	539 (2.94)
S_Shelf	16357	338 (2.07)	474 (2.90)
Open sea	129495	3442 (2.66)	5109 (3.95)

Hypermethylation and hypomethylation were calculated using a Bonferroni-adjusted *P*-value <0.05 and an *M*-value cutoff of 1.

Functional annotation tools for hypomethylated regulatory regions in schwannomas using DAVID (excluding those CpGs on gene bodies) showed enrichment in terms of axon projection, Semaplexin domains, HOX sequence, apoptosis, and Ras/rho signaling (Supporting Information Table 2). Hypermethylated regulatory regions were enriched in cell motility, adhesion, and cytoskeleton.

Gene Methylation Patterns

To compare the genes with altered methylated patterns in vestibular schwannoma and controls, we grouped the microarray probes into the six categories before use for each transcript (TSS1500, TSS200, 5′UTR, first exon, gene body, and 3′UTR) with the IMA *regionswrapper* function. Hypomethylation was more frequent than hypermethylation in the tumors (849 vs. 562 genes). By a significant margin, the region showing the largest number of altered genes in both hypomethylation and hypermethylation was 3′UTR. The 344 hypomethylated genes in this 3′UTR region included *MTOR*, *HOXD4*, *PAX8*, and *SOX8*, while the 152 hypermethylated genes included *SOX1*, *ROBO4*, and *NEU4*. The next region with the largest number of alterations was the gene body, with 127 hypomethylated genes including *EVI2A*, *HOXD4*, *CTNND1*, and *PMP2* and 106 aberrant methylated genes including *VSTM1*, *NDEL1*, and *ESM1*. *EVI2A* is located within an intron of *NF1*, but this gene showed no epigenetic alteration. First exon hypomethylation was found in 75 genes (such as *PMP2*, *MBP*, and *MOG*) and was similar to hypermethylation in 73 genes (including *S100P*, *SOX1*, and *IGF1*). Region 5′UTR showed the lowest number of total altered genes with 127; 60 of them displayed hypermethylation (e.g., *HOXD3*, *S100B*, and *HEPACAM*) and 67 presented hypomethylation (e.g., *APOL4* and *IGF1*). Finally, TSS regions had 407 altered genes, displaying 236 hypomethylated genes (such as *TP63*, *TNF*, *CTNND1*, and *S100A2*) and 171 hypermethylated genes (including

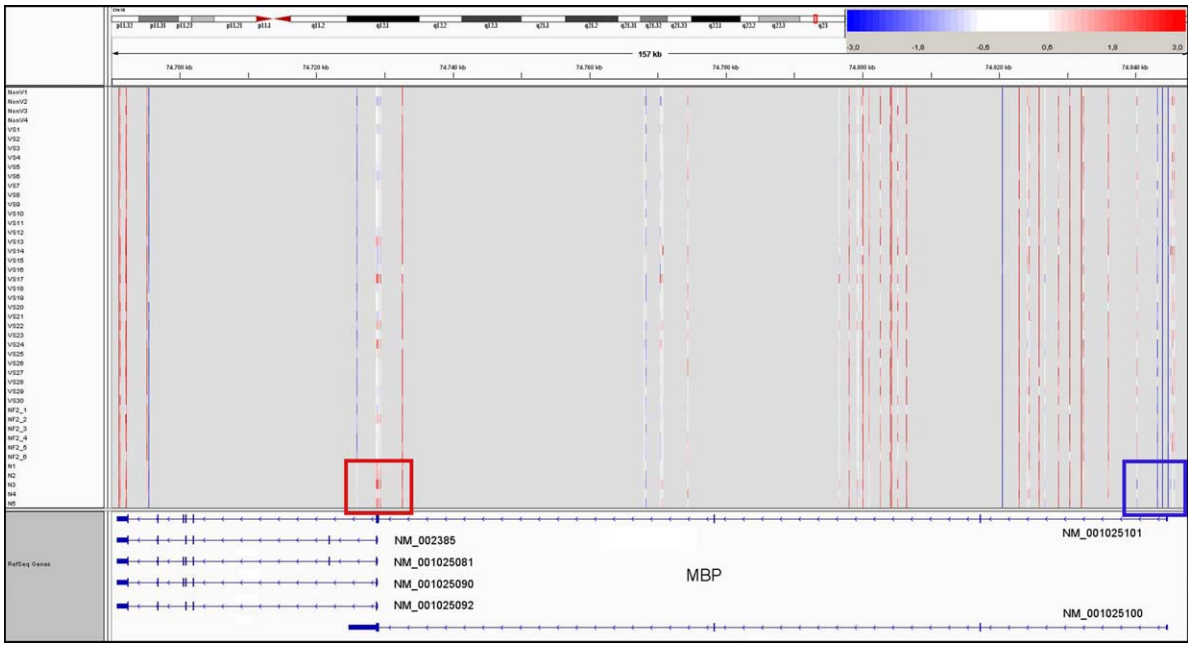

Figure 2. *MBP* gene methylation pattern. Long isoform promoter regions NM_001025100 and NM_001025101 were hypermethylated in schwannomas at CpG sites (blue box), while short isoforms NM_001025090, NM_002385, NM_001025092, and NM_001025081 were hypomethylated (red box).

ITGAE, *FOXD2* and *TFAP2A*). Full results are shown in Supporting Information Table 3.

At the single CpG level, we also searched for genes showing several probes with aberrant methylation patterns. Since Schwann cells contribute to the insulation of axons by myelin (a lipid covering), we searched for genes involved in myelination and lipid processes. We found a set of these genes to be altered, including *MBP*, *PMP2*, *G0S2*, *FABP7*, *OSBPL5*, *CNP*, *APOB*, and *MOG*. The *NF2* gene did not present any differentially methylated probe in either the vestibular or nonvestibular tumors using this microarray.

We used our previously published gene expression study of vestibular schwannomas to find altered methylation patterns that coincided with the expected deregulation observed in expression (hypermethylation underexpression or hypomethylation overexpression). In both altered epigenetic patterns, genes with these alterations were more extensive than those with a noncanonical epigenetic expression pattern. Given that the involvement of the gene body and 3′UTR methylation in gene expression is controversial, we only considered TSS1500, TSS200, 5′UTR, and first exon regions for this purpose. The upregulated and hypomethylated genes included *MET*, *CX3CR1*, *HEPACAM*, *PMP2*, and *MERTK* (Supporting Information Table 4). The downregulated and hypermethylated genes included *CD177*, *MFAP5*, *G0S2*, *AQP9*, and *VIT* (Supporting Information Table 5).

Global HOX Genes Hypomethylation

Numerous HOX genes, which participate in body plan development, showed a differential methylation pattern, in most cases hypomethylation in schwannomas. The HOXD cluster, located at chromosome 2q, showed *HOXD1*, *HOXD3*, *HOXD4*, *HOXD8*, and *HOXD9* to be clearly hypomethylated in 35 probes, as shown in Figure 1. The HOXA cluster, located at chromosome 7p, also had this pattern in a total of 27 probes in *HOXA3*, *HOXA4*, and *HOXA6*. In the HOXB cluster, at 17q, 15 CpG sites were hypomethylated (including *HOXB1* and *HOXB3*), and three were hypermethylated, two of them at the *HOXB2* gene. Finally, cluster HOXC, at chromosome 12q, had 16 hypomethylated probes, mainly at *HOXC4*. *MEIS1*, *MEIS2*, *PBX1*, and *PBX2* (Hox gene cofactors) presented differential methylation patterns in 19, 10, 8, and 2 CpG sites, respectively, most located at the gene body. The MEIS cofactors showed hypermethylation while the PBX cofactors presented hypomethylation, except in 4 CpG sites of *PBX1*.

Gene Methylation and Alternative Splicing

A set of genes showed varying methylation levels along CpG sites included within the gene, that is, several CpGs were hypomethylated and others were hypermethylated. This variation might lead to alternative transcription. In the *MBP* gene, 3 CpG at 5′UTR and TSS sites of isoforms NM_001025100 and NM_001025101 were hypermethylated in schwannomas, while smaller isoforms (NM_001025090, NM_002385, NM_001025092, and NM_001025081) were clearly hypomethylated at 13 CpG sites within regulatory regions as shown in Figure 2. Thus, *MBP* might present alternative isoform expression. Gene *ZNF238* (ZBTB18) showed hypermethylation in four probes in the NM_205768 isoform on the TSS region; while hypomethylation was found in another four probes at the body gene of this isoform in the tumors, which coincides with the first exon of isoform NM_006352. Therefore, if a canonical methylation mechanism operated on this gene, the last isoform would have a greater probability of being transcribed.

The single CpG site-specific methylation suggested relevant changes related to DNA epigenetic differences within the gene and alternative isoform expression based on our results. An example of a gene that could be affected by this mechanism is *NRXN1*. A total of 17 CpGs were differentially methylated in this gene; 10 of them were hypomethylated and seven were hypermethylated in schwannomas. Through the analysis of expression arrays at the exon level, we previously found an NM_138735 transcript of this gene with no expression level changes, while NM_004801 was overexpressed in the tumors. Interestingly, hypomethylation was found in those CpG sites included in NM_004801 at the gene body and hypermethylation in probes also shared with NM_138735, mainly in the regulatory regions. A diagram of this process is shown in Figure 3.

Methylation Pattern in miRNAs

A total of 68 CpG sites located at miRNAs were hypomethylated in vestibular schwannomas, some of them with several affected CpG site probes, such as miR-10b and miR-1204. Hypermethylation in miRNAs occurred in 73 CpGs, including miR-596, miR-199a1, and miR-185. The miRNA-548 family was the most deregulated at the methylation level, with 19 probes altered. Of these probes, 11 were hypermethylated, 8 of which corresponded to miR-548f5, and 2 to miR-548n. The miR-548f5 gene also had two hypomethylated sites. The miRNA-548h4 displayed one CpG hypomethylated site and another site was hypermethylated. Using our previously published studies on miRNA expression profile in schwannomas, we found that methylation patterns generally corresponded to what was expected (hypermethylation as repressor). Examples of hypomethylation and upregulation include miR-21 (5 probes) and miR-145 (3 probes). Hypermethylation and repression were found in miR-199a1 at 5 probes and miR-185 at 2 probes.

Discrepancies with Canonical Expectations in Methylation and Expression

A set of genes presented an expression pattern that was not expected from the results obtained by methylation. An example was the *PDGFA* gene, which was hypermethylated in a single CpG at the TSS1500 promoter region and hypomethylated in the gene body, while it was upregulated in tumors. In the case of miR-10b (included in the HOXD cluster), the expected methylation and expression pattern was once again not found. MiRNA-10b presented hypomethylation of 10 CpGs sites, although in the expression study it was found to be clearly downregulated.

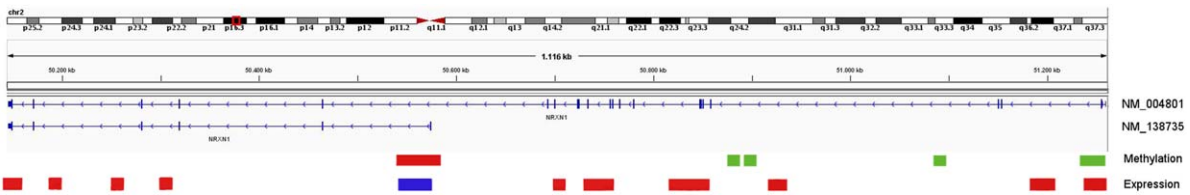

Figure 3. Neurexin-1 might present alternative splicing in schwannomas. Two isoforms of the *NRXN1* gene are shown. Long transcript NM_004801 shows overexpression (in red) and hypomethylation (in green). Transcript NM_138735 shows overexpression in probes shared with the long isoform and no changes in expression in those probes specifically for the short form. Additionally, the methylation pattern is increased in the region belonging to the promoter region of this isoform.

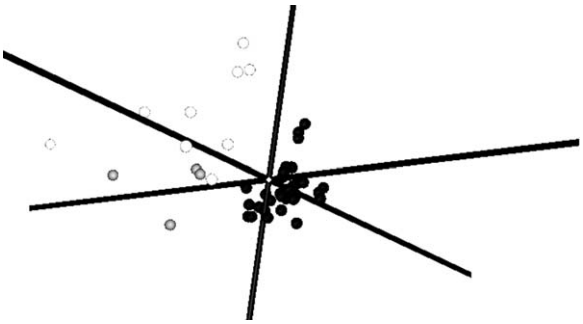

Figure 4. HOX gene expression represented by PCA. All probes available in Gene 1.0ST array at the exon level for HOX genes were used in this data-reduction approach. Control nerves (white dots) and nonvestibular schwannomas (gray) suggest a different pattern of expression than vestibular tumors (black).

Nonvestibular Schwannomas

We tested four nonvestibular schwannoma cases with Infinium microarrays and established a list of 212 CpG sites that were differentially methylated with respect to the vestibular tumors. Of these 212 CpG sites, 88 corresponded to HOX clusters genes, which are usually hypermethylated in nonvestibular schwannomas. Additionally, *SOX1* was hypomethylated at 3 CpG sites in nonvestibular schwannomas, while *SOX2* (at 7 CpGs) appeared hypermethylated with respect to vestibular tumors. We wanted to know whether the expression patterns of HOX genes were also altered, thus we performed an mRNA expression microarray assay for those four cases. We found that, in the exon-level expression analysis, PCA of all probes available for HOX genes separated vestibular and nonvestibular schwannomas as shown in Figure 4. Thus, the methylation and expression patterns of HOX and related genes seem to be similar in native nerves and nonvestibular schwannomas and are altered in vestibular tumors.

Clinical and Molecular Comparisons

We searched for CpG sites with differential methylation between schwannomas by using molecular and clinical data collected from patients at our institution. Sporadic vs. NF2-vestibular schwannomas showed 123 sites with differential methylation, including hypomethylation of *DIP2C*, while *WDR66*, and *PTPRN2* were hypermethylated in 2 CpG sites each in the samples originating from NF2 patients. By tumor location (side), 1 CpG was detected. By gender, 26 probes were found in autosomes, several of them with very low *P*-values and high fold-changes, such as the *TLE1* gene at 3 CpG sites, which was hypermethylated in females. This outcome suggests that, as previously reported (Chen et al., 2013), this array might show some degree of gender bias. However, the low number of probes with this problem suggests that it was not an important issue in our data. All of the data are presented in Supporting Information Table 6. Other clinical features tested without any probe with aberrant methylation included the schwannoma type (homogeneous, heterogeneous

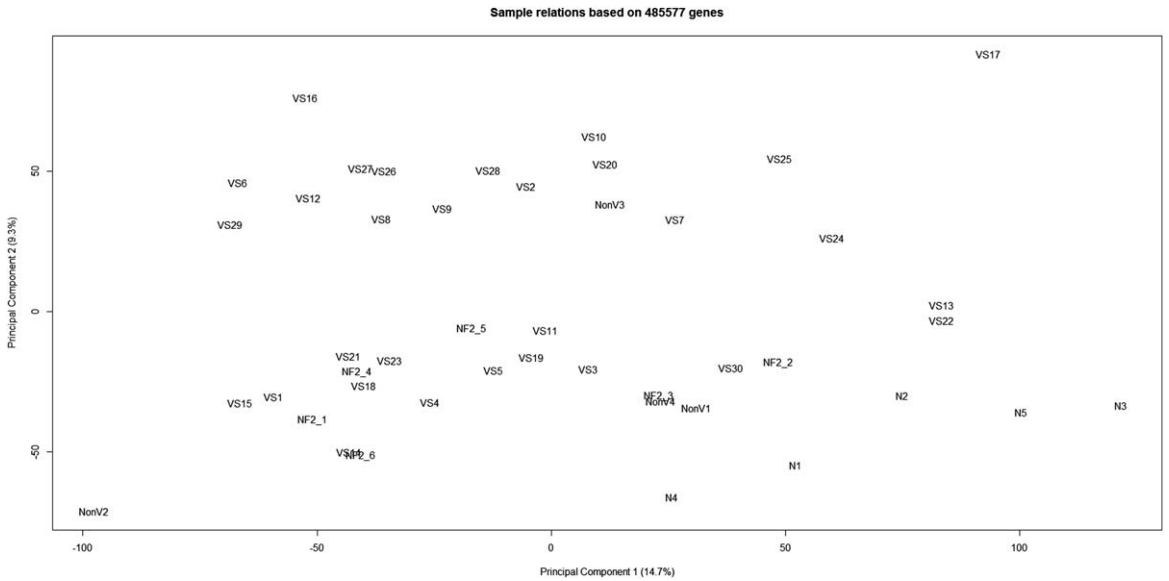

Figure 5. Principal component analysis of samples. Whole CpG sites were used to generate this graphical representation. Control nerves (N) were grouped outside tumors. Neither nonvestibular tumors nor NF2-vestibular schwannomas seemed to present differential behavior in overall CpG representation. Control nerves are grouped in the right corner.

or cystic), tumor size (Koos 1 and 2 vs. Koos 3 and 4), smoking habits, presence of tinnitus prior to surgery, tumor pressure upon the pons, dizziness before surgery, whether the tumor reached IAC and whether facial conduction after surgery was less or equal at 0.05 mA. Moreover, PCA of all samples showed no apparent association among tumors based on their origin, as shown in Figure 5.

A mutational analysis of *NF2* showed that 55% of samples had sequence alterations, whereas rearrangements detected by MLPA presented in 25% of cases, and LOH at 22q was identified in 62% of the tumors (Supporting Information Table 7). Overall, 75% of the samples had at least one hit detected in the *NF2* gene. Every class was tested: sequence alteration versus not found; MLPA normal versus altered, normal constitution at 22q versus LOH; and samples with no hits in NF2 versus at least one hit. When this last class comparison was performed, a subset of 32 CpGs displayed alterations. Of these, *MAFK* (at 7p) was hypermethylated at 2 CpG sites in those tumors with no *NF2* alterations. The other classes showed no differences.

DISCUSSION

Schwannomas are benign neoplasms that arise from Schwann cells. Although genetic alterations have been investigated in this neoplasm, few studies are available on the epigenetic changes in schwannomas. In this study, we analyzed the epigenetic signature of individual CpG methylation among 36 vestibular schwannomas, 4 nonvestibular schwannomas, and 5 healthy control samples of nerve tissue using microarray technology.

CpG islands, where cytosine is more abundant, showed a lower percentage of change via hypomethylation or aberrant methylation in schwannomas, not reaching 1%. In fact, flanking zones such as CpG shores, shelves and open sea presented increased numbers of changes (in relative levels). Thus, differential methylation levels between schwannomas and controls seem to increase as the distance from CpG islands increases. Non-CpG Island methylation, mainly at shores, has been identified as paramount in the regulation of numerous genes in cell reprogramming (Doi et al., 2009), in the classification of various tissues (Kozlenkov et al., 2014) and in cancer (Rao et al., 2013). Overall, hypomethylation and hypermethylation levels were similar, with a trend toward hypomethylation as previously described for colon cancer (Irizarry et al., 2009) but in contraposition for hepatocellular carcinoma, where methylation was clearly biased toward hypomethylation (Shen et al., 2013). These differences among studies might be due to intrinsic tumor characteristics.

One of the most significant results was global hypomethylation (with few gene exceptions) of the four HOX gene clusters in vestibular schwannomas. These genes are involved in morphological changes and animal body plan evolution. HOX aberrant expression in tumoral tissue compared to control tissues (Abate-Shen 2002) has been linked to multiples types of cancer such as pancreatic cancer (Cantile et al., 2009), hepatocellular carcinoma (Cillo et al., 2011), and leukemia (Argiropoulos and Humphries 2007). This alteration has also been identified as a prognostic factor in meningiomas (Di Vinci et al., 2012) and thyroid cancer (Cantile et al., 2013). Moreover, the HOX cofactor proteins *MEIS* and *PBX* also experienced DNA methylation variations. Nonvestibular schwannomas displayed a different methylation profile in regard to HOX genes and cofactors, which was more similar to that found in nerves. The PCA of mRNA expression assay also distinguished between those tumors (Fig. 4). Nonvestibular schwannomas harbor *BRAF* mutations at a low rate, but this does not occur in vestibular schwannomas (de Vries et al., 2013), suggesting that there might be specific molecular signatures between the two neoplasms. Nonetheless, our results show that the methylation pattern of nonvestibular and vestibular schwannomas was very similar in the rest of CpG sites, given that no differences were found when the whole CpG probes were compared by PCA (Fig. 5). Overall, our results suggest that HOX genes could play an important role in vestibular schwannomas but do not seem to be involved in nonvestibular tumors, although the low number of cases presented here (of nonvestibular tumors) warrants additional experiments in this regard. Thus, we propose that, based on the numerous tumor types affected by deregulation of HOX genes, this group of genes might be of interest for a potential treatment in vestibular schwannoma, although it needs further study, as it is not clear whether HOX deregulation is a cause or an effect in carcinogenesis (Bhatlekar et al., 2014).

Gene expression changes are one of the most studied consequences of CpG methylation. This relationship has been highlighted in tissue specificity (Lokk et al., 2014), differentiation (Liu et al., 2014), cancer development (Dammann et al., 2000) and recurrence (Tsunedomi et al., 2013). In our study, the correlations between gene

expression and DNA methylation were in general negative, that is, hypomethylated and overexpressed, although there was a small fraction of genes that exhibited aberrant methylation overexpression or hypomethylation underexpression. This result has also been observed in other studies, (Dayeh et al., 2014) suggesting that CpG sites methylation, even at promoter regions (at TSS, 5′UTR and first exon) is important but not decisive in gene expression. Although a single CpG has been shown to be able to produce gene silencing (Zhang et al., 2010), we centered our wide-methylation analysis on those genes with more than one altered CpG.

PMEPA1 displayed seven CpG sites to be hypomethylated, all corresponding to promoter regions. With mRNA overexpressed in schwannomas, this gene regulates androgen receptor (*AR*) levels, which is also downregulated in this neoplasm (Torres-Martin et al., 2013a, 2013b). Epigenetic processes in *PMEPA1* regulation have been described in prostate cancer (Richter et al., 2007). Therefore, *PMEPA1* hypomethylation might lead to its overexpression and, as a consequence, to AR silencing. The effect of *AR* downregulation in schwannomas is not clear. A possibility might be linked to the interaction with caveolin-1, a gene that is also downregulated in this tumor. *CAV1* has been described as an *AR* coactivator in prostate cancer cell lines (Wu and Terrian 2002; Bennett et al., 2014).

Another hypomethylated gene was *MET* oncogene, which presented two hypomethylated CpG sites at the promoter region and overexpressed mRNA. MET is a tyrosine kinase receptor that controls various functions including proliferation and migration. Phosphoprotein levels of MET have been reported in schwannomas, indicating that it is present in tumors (Boin et al., 2014). *MET* expression linked to promoter epigenetic regulation has been described in other oncogenic processes such as the metastasis of hepatocellular carcinoma (Ogunwobi et al., 2013). Thus, *MET* gene mRNA overexpression might occur in schwannomas through epigenetic mechanisms.

Schwannomas showed a set of genes related to myelination processes with altered epigenetic signatures, including *MBP* and *PMP2*. Changes in these genes were also found in an immunohistochemistry study (Hung et al., 2002) and expression analysis (Torres-Martin et al., 2013a, 2013b). In the latter study, a developmental state between the neural crest and Schwann cell precursor was suggested. Thus, methylation seems to play an important role in processes related to myelin formation in schwannomas, possibly exhibiting epigenetic changes leading to dedifferentiation. Based on our data, the *NF2* gene does not seem to be affected by methylation processes in schwannomas, in agreement with Koutsimpelas et al., (2012) and Lee et al., (2012), although methylation in a small subset of samples should not be ruled out (Gonzalez-Gomez et al., 2003; Kullar et al., 2010). Additionally, the *NF1* gene, which is involved in neurofibromatosis Type 1 (NF1) syndrome, contains a small gene within an intron named *EVI2A*. In 2 *EVI2A* CpG sites, hypomethylation was detected. This finding agrees with the overexpression of *EVI2A* found in schwannomas (Torres-Martin et al., 2013a, 2013b) and with that described in head and neck cancer (Poage et al., 2011). Thus, there might be a connection between both neurofibromatosis types (NF1 and NF2) via this gene; however, the mechanism remains elusive.

MiRNAs presented changes in DNA methylation pattern at the promoter and body regions. Numerous epigenetic mechanisms that modify the expression level of these small molecules have been found (Lopez-Serra and Esteller 2012). Furthermore, miRNAs are epigenetically altered in tumors such as oral cancer (Kozaki et al., 2008), acute lymphoblastic leukemia (Agirre et al., 2009), colorectal carcinogenesis (Balaguer et al., 2010), and hepatocellular carcinoma (Furuta et al., 2010). In our tumor series, miR-21 was hypomethylated in 5 CpG sites, three of which corresponded to promoter regions. As expected, miR-21 expression level was found to be clearly upregulated, in the same manner as other tumors, such as hepatocellular carcinoma (Xu et al., 2013) and gastric cancer (Zhang et al., 2012). Conversely, miRNA-199a1 was hypermethylated and downregulated. MiRNA-199a1 targets MET (Kim et al., 2008) and thus the downregulation of this miRNA could participate in *MET* overexpression. Additionally, despite having several hypomethylated CpG sites, several miRNAs exhibited downregulation. This process was very pronounced in miR-10b, with 10 CpG sites hypomethylated and with a clear downregulation in schwannomas. Given that eight of these CpG are located within the *HOXD4* gene, there might be other mechanisms leading to this transcript downregulation. MiRNA hypomethylation and underexpression has also been previously reported (Liu et al., 2014), suggesting that, although CpG methylation at miRNAs genes usually follows the expected pattern of action, this phenomenon is not completely able to predict the behavior of a particular miRNA.

Currently, body methylation does not have an obvious role in gene expression. Proposed models include a reduction of transcriptional noise (Huh et al., 2013), alternative splicing (Maunakea et al., 2010) and even transcription regulation but in a different manner than in promoters, with overexpressed and underexpressed genes having moderate methylation levels (Su et al., 2014). In our study, we detected various transcripts belonging to the same gene but not showing the same methylation pattern. Thus, we found neurexin-1 with hypomethylation and hypermethylation of distinct transcripts, as confirmed by mRNA expression. This gene, which is able to generate hundreds of alternative transcripts (Ushkaryov et al., 1992), is involved in the formation of synapses and in the vascular system (Melani and Weinstein 2010). Therefore, based on the specific methylation pattern of various isoforms, the picture of methylation expression in schwannomas significantly increases in complexity, because changes in methylation would not only be limited to changes in the expression of a specific gene but also in a subtle regulation of alternative transcripts, as described in human colon cancer for the VEGF gene (Hamdollah Zadeh et al. 2014). The consequences of this fact might be of great importance, as treatment options could not only be limited to the silencing of an aberrant expressed gene, but to restoring the levels of the nonpathological isoform.

In agreement with our previous expression analysis, we found no significant differences between vestibular schwannomas regarding clinical or molecular features in an epigenetic context. Nevertheless, a small subset of CpG sites were identified and could be a signature of certain subtypes, such as hypermethylated *MAFK* at 2 CpG sites in those vestibular schwannomas with no detected *NF2* hits.

In conclusion, schwannoma CpG site-specific signatures compared to nontumoral nerves show a trend toward hypomethylation. CpG islands seem to be less involved in epigenetic changes than shores, shelves and open sea. Furthermore, expression levels were altered in several genes where hypo or hypermethylation was present at the promoter region, including *MET* and *PMEPA1*. Moreover, we have identified a possible mechanism of expression in alternative transcripts in neurexin-1. We also report that *EVI2A* (located at the *NF1* gene intron) might be upregulated in tumors by hypomethylation. Finally, we detected HOX gene cluster global hypomethylation in vestibular schwannoma, but no changes in these genes were found in nonvestibular tumor cases, suggesting that treatment options for schwannomas from a variety of places might require different approaches.

ACKNOWLEDGMENTS

The authors would like to thank Carolina Peña-Granero for her excellent technical assistance. The authors declare no conflicts of interest.

REFERENCES

Aarhus M, Bruland O, Sætran HA, Mork SJ, Lund-Johansen M, Knappskog PM. 2010. Global gene expression profiling and tissue microarray reveal novel candidate genes and down-regulation of the tumor suppressor gene CAV1 in sporadic vestibular schwannomas. Neurosurgery 67:998–1019.

Abate-Shen C. 2002. Deregulated homeobox gene expression in cancer: Cause or consequence? Nat Rev Cancer 2:777–785.

Agirre X, Vilas-Zornoza A, Jiménez-Velasco A, Martin-Subero JI, Cordeu L, Gárate L, San José-Eneriz E, Abizanda G, Rodríguez-Otero P, Fortes P, Rifón J, Bandrés E, Calasanz MJ, Martín V, Heiniger A, Torres A, Siebert R, Román-Gomez J, Prósper F. 2009. Epigenetic silencing of the tumor suppressor microRNA Hsa-miR-124a regulates CDK6 expression and confers a poor prognosis in acute lymphoblastic leukemia. Cancer Res 69:4443–4453.

Argiropoulos B, Humphries RK. 2007. Hox genes in hematopoiesis and leukemogenesis. Oncogene 26:6766–6776.

Balaguer F, Link A, Lozano JJ, Cuatrecasas M, Nagasaka T, Boland CR, Goel A. 2010. Epigenetic silencing of miR-137 is an early event in colorectal carcinogenesis. Cancer Res 70: 6609–6618.

Bello MJ, de Campos JM, Kusak ME, Vaquero J, Sarasa JL, Pestaña A, Rey JA. 1993. Clonal chromosome aberrations in neurinomas. Genes Chromosomes Cancer 6:206–211.

Bello MJ, Martinez-Glez V, Franco-Hernandez C, Pefla-Granero C, de Campos JM, Isla A, Lassaletta L, Vaquero J, Rey JA. 2007. DNA methylation pattern in 16 tumor-related genes in schwannomas. Cancer Genet Cytogenet 172:84–86.

Bennett NC, Hooper JD, Johnson DW, Gobe GC. 2014. Expression profiles and functional associations of endogenous androgen receptor and caveolin-1 in prostate cancer cell lines. Prostate 74:478–487.

Bhatlekar S, Fields JZ, Boman BM. 2014. HOX genes and their role in the development of human cancers. J Mol Med (Berl) 92:811–823.

Boin A, Couvelard A, Couderc C, Brito I, Filipescu D, Kalamarides M, Bedossa P, De Koning L, Danelsky C, Dubois T, Hupé P, Louvard D, Lallemand D. 2014. Proteomic screening identifies a YAP-driven signaling network linked to tumor cell proliferation in human schwannomas. Neuro-Oncol 16: 1196–1209.

Cantile M, Franco R, Tschan A, Baumhoer D, Zlobec I, Schiavo G, Forte I, Bihl M, Liguori G, Botti G, Tornillo L, Karamitopoulou-Diamantis E, Terracciano L, Cillo C. 2009. HOX D13 expression across 79 tumor tissue types. Int J Cancer 125:1532–1541.

Cantile M, Scognamiglio G, La Sala L, La Mantia E, Scaramuzza V, Valentino E, Tatangelo F, Losito S, Pezzullo L, Chiofalo MG, Fulciniti F, Franco R, Botti G. 2013. Aberrant expression of posterior HOX genes in well differentiated histotypes of thyroid cancers. Int J Mol Sci 14:21727–21740.

Chen Y, Lemire M, Choufani S, Butcher DT, Grafodatskaya D, Zanke BW, Gallinger S, Hudson TJ, Weksberg R. 2013. Discovery of cross-reactive probes and polymorphic CpGs in the Illumina Infinium HumanMethylation450 microarray. Epigenetics 8:203–209.

Cillo C, Schiavo G, Cantile M, Bihl MP, Sorrentino P, Carafa V, D' Armiento M, Roncalli M, Sansano S, Vecchione R, Tornillo L, Mori L, De Libero G, Zucman-Rossi J, Terracciano L. 2011. The HOX gene network in hepatocellular carcinoma. Int J Cancer 129:2577–2587.

Dammann R, Li C, Yoon JH, Chin PL, Bates S, Pfeifer GP. 2000. Epigenetic inactivation of a RAS association domain family protein from the lung tumour suppressor locus 3p21.3. Nat Genet 25:315–319.

Dayeh T, Volkov P, Salö S, Hall E, Nilsson E, Olsson AH, Kirkpatrick CL, Wollheim CB, Eliasson L, Rönn T, Bacos K, Ling C. 2014. Genome-wide DNA methylation analysis of human pancreatic islets from type 2 diabetic and non-diabetic donors identifies candidate genes that influence insulin secretion. PLoS Genet 10:e1004160.

de Vries M, Bruijn IB, Cleton-Jansen A-M, Malessy MJA, van der Mey AGL, Hogendoorn PCW. 2013. Mutations affecting BRAF, EGFR, PIK3CA, and KRAS are not associated with sporadic vestibular schwannomas. Virchows Arch 462:211–217.

Di Vinci A, Brigati C, Casciano I, Banelli B, Borzì L, Forlani A, Ravetti GL, Allemanni G, Melloni I, Zona G, Spaziante R, Merlo DF, Romani M. 2012. HOXA7, 9, and 10 are methylation targets associated with aggressive behavior in meningiomas. Transl Res 160:355–362.

Doherty JK, Ongkeko W, Crawley B, Andalibi A, Ryan AF. 2008. ErbB and Nrg: Potential molecular targets for vestibular schwannoma pharmacotherapy. Otol Neurotol 29:50–57.

Doi A, Park I-H, Wen B, Murakami P, Aryee MJ, Irizarry R, Herb B, Ladd-Acosta C, Rho J, Loewer S, Miller J, Schlaeger T, Daley GQ, Feinberg AP. 2009. Differential methylation of tissue- and cancer-specific CpG island shores distinguishes human induced pluripotent stem cells, embryonic stem cells and fibroblasts. Nat Genet 41:1350–1353.

Du P, Kibbe WA, Lin SM. 2008. lumi: A pipeline for processing Illumina microarray. Bioinformatics 24:1547–1548.

Du P, Zhang X, Huang C-C, Jafari N, Kibbe WA, Hou L, Lin SM. 2010. Comparison of Beta-value and M-value methods for quantifying methylation levels by microarray analysis. BMC Bioinformatics 11:587.

Esteller M, Garcia-Foncillas J, Andion E, Goodman SN, Hidalgo OF, Vanaclocha V, Baylin SB, Herman JG. 2000. Inactivation of the DNA-repair gene MGMT and the clinical response of gliomas to alkylating agents. N Engl J Med 343:1350–1354.

Furuta M, Kozaki K, Tanaka S, Arii S, Imoto I, Inazawa J. 2010. miR-124 and miR-203 are epigenetically silenced tumor-suppressive microRNAs in hepatocellular carcinoma. Carcinogenesis 31:766–776.

Gonzalez-Gomez P, Bello MJ, Alonso ME, Lomas J, Arjona D, de Campos JM, Vaquero J, Isla A, Lassaletta L, Gutierrez M, Sarasa JL, Rey JA. 2003. CpG island methylation in sporadic and neurofibromatis type 2-associated schwannomas. Clin Cancer Res 9:5601–5606.

Hamdollah Zadeh MA, Amin EM, Hoareau-Aveilla C, Domingo E, Symonds KE, Ye X, Heesom KJ, Salmon A, D'Silva O, Betteridge KB, Williams AC, Kerr DJ, Salmon AHJ, Oltean S, Midgley RS, Ladomery MR, Harper SJ, Varey AHR, Bates DO. 2014. Alternative splicing of TIA-1 in human colon cancer regulates VEGF isoform expression, angiogenesis, tumour growth and bevacizumab resistance. Mol Oncol (in press) http://dx.doi.org/10.1016/j.molonc.2014.07.017.

Huang DW, Sherman BT, Lempicki RA. 2009. Systematic and integrative analysis of large gene lists using DAVID bioinformatics resources. Nat Protoc 4:44–57.

Huh I, Zeng J, Park T, Yi SV. 2013. DNA methylation and transcriptional noise. Epigenetics Chromatin 6:9.

Hung G, Colton J, Fisher L, Oppenheimer M, Faudoa R, Slattery W, Linthicum F. 2002. Immunohistochemistry study of human vestibular nerve schwannoma differentiation. Glia 38:363–370.

Irizarry RA, Ladd-Acosta C, Wen B, Wu Z, Montano C, Onyango P, Cui H, Gabo K, Rongione M, Webster M, Ji H, Potash JB, Sabunciyan S, Feinberg AP. 2009. The human colon cancer methylome shows similar hypo- and hypermethylation at conserved tissue-specific CpG island shores. Nat Genet 41:178–186.

Johnson WE, Li C, Rabinovic A. 2007. Adjusting batch effects in microarray expression data using empirical Bayes methods. Biostatistics 8:118–127.

Karajannis MA, Legault G, Hagiwara M, Giancotti FG, Filatov A, Derman A, Hochman T, Goldberg JD, Vega E, Wisoff JH, Golfinos JG, Merkelson A, Roland JT, Allen JC. 2014. Phase II study of everolimus in children and adults with neurofibromatosis type 2 and progressive vestibular schwannomas. Neuro Oncol 16:292–297.

Kim S, Lee UJ, Kim MN, Lee E-J, Kim JY, Lee MY, Choung S, Kim YJ, Choi Y-C. 2008. MicroRNA miR-199a* regulates the MET proto-oncogene and the downstream extracellular signal-regulated kinase 2 (ERK2). J Biol Chem 283:18158–18166.

Kino T, Takeshima H, Nakao M, Nishi T, Yamamoto K, Kimura T, Saito Y, Kochi M, Kuratsu J, Saya H, Ushio Y. 2001. Identification of the cis-acting region in the NF2 gene promoter as a potential target for mutation and methylation-dependent silencing in schwannoma. Genes Cells 6:441–454.

Koutsimpelas D, Ruerup G, Mann WJ, Brieger J. 2012. Lack of neurofibromatosis type 2 gene promoter methylation in sporadic vestibular schwannomas. ORL J Otorhinolaryngol Relat Spec 74:33–37.

Kozaki K, Imoto I, Mogi S, Omura K, Inazawa J. 2008. Exploration of tumor-suppressive microRNAs silenced by DNA hypermethylation in oral cancer. Cancer Res 68:2094–2105.

Kozlenkov A, Roussos P, Timashpolsky A, Barbu M, Rudchenko S, Bibikova M, Klotzle B, Byne W, Lyddon R, Di Narzo AF, Hurd YL, Koonin EV, Dracheva S. 2014. Differences in DNA methylation between human neuronal and glial cells are concentrated in enhancers and non-CpG sites. Nucleic Acids Res 42:109–127.

Kullar PJ, Pearson DM, Malley DS, Collins VP, Ichimura K. 2010. CpG island hypermethylation of the neurofibromatosis type 2 (NF2) gene is rare in sporadic vestibular schwannomas. Neuropathol Appl Neurobiol 36:505–514.

Lee JD, Kwon TJ, Kim U-K, Lee W-S. 2012. Genetic and epigenetic alterations of the NF2 gene in sporadic vestibular schwannomas. PloS One 7:e30418.

Li W, You L, Cooper J, Schiavon G, Pepe-Caprio A, Zhou L, Ishii R, Giovannini M, Hanemann CO, Long SB, Erdjument-Bromage H, Zhou P, Tempst P, Giancotti FG. 2010. Merlin/NF2 suppresses tumorigenesis by inhibiting the E3 ubiquitin ligase CRL4(DCAF1) in the nucleus. Cell 140:477–490.

Liu Z, Jiang R, Yuan S, Wang N, Feng Y, Hu G, Zhu X, Huang K, Ma J, Xu G, Liu Q, Xue Z, Fan G. 2014. Integrated analysis of dna methylation and rna transcriptome during in vitro differentiation of human pluripotent stem cells into retinal pigment epithelial cells. PloS One 9:e91416.

Lokk K, Modhukur V, Rajashekar B, Märtens K, Mägi R, Kolde R, Kolt Ina M, Nilsson TK, Vilo J, Salumets A, Tõnisson N. 2014. DNA methylome profiling of human tissues identifies global and tissue-specific methylation patterns. Genome Biol 15:R54.

Lopez-Serra P, Esteller M. 2012. DNA methylation-associated silencing of tumor-suppressor microRNAs in cancer. Oncogene 31:1609–1622.

Mack SC, Witt H, Piro RM, Gu L, Zuyderduyn S, Stütz AM, Wang X, Gallo M, Garzia L, Zayne K, Zhang X, Ramaswamy V, Jäger N, Jones DTW, Sill M, Pugh TJ, Ryzhova M, Wani KM, Shih DJH, Head R, Remke M, Bailey SD, Zichner T, Faria CC, Barszczyk M, Stark S, Seker-Cin H, Hutter S, Johann P, Bender S, Hovestadt V, Tzaridis T, Dubuc AM, Northcott PA, Peacock J, Bertrand KC, Agnihotri S, Cavalli FMG, Clarke I, Nethery-Brokx K, Creasy CL, Verma SK, Koster J, Wu X, Yao Y, Milde T, Sin-Chan P, Zuccaro J, Lau L, Pereira S, Castelo-Branco P, Hirst M, Marra MA, Roberts SS, Fults D, Massimi L, Cho YJ, Van Meter T, Grajkowska W, Lach B, Kulozik AE, von Deimling A, Witt O, Scherer SW, Fan X, Muraszko KM, Kool M, Pomeroy SL, Gupta N, Phillips J, Huang A, Tabori U, Hawkins C, Malkin D, Kongkham PN, Weiss WA, Jabado N, Rutka JT, Bouffet E, Korbel JO, Lupien M, Aldape KD, Bader GD, Eils R, Lichter P, Dirks PB, Pfister SM, Korshunov A, Taylor MD. 2014. Epigenomic alterations define lethal CIMP-positive ependymomas of infancy. Nature 506:445–450.

Maunakea AK, Nagarajan RP, Bilenky M, Ballinger TJ, D'Souza C, Fouse SD, Johnson BE, Hong C, Nielsen C, Zhao Y, Turecki G, Delaney A, Varhol R, Thiessen N, Shchors K, Heine VM, Rowitch DH, Xing X, Fiore C, Schillebeeckx M, Jones SJM, Haussler D, Marra MA, Hirst M, Wang T, Costello JF. 2010. Conserved role of intragenic DNA methylation in regulating alternative promoters. Nature 466:253–257.

Melani M, Weinstein BM. 2010. Common factors regulating patterning of the nervous and vascular systems. Annu Rev Cell Dev Biol 26:639–665.

Mur P, Mollejo M, Ruano Y, de Lope ÁR, Fiaño C, García JF, Castresana JS, Hernández-Laín A, Rey JA, Meléndez B. 2013. Codeletion of 1p and 19q determines distinct gene methylation and expression profiles in IDH-mutated oligodendroglial tumors. Acta Neuropathol (Berl) 126:277–289.

Ogunwobi OO, Puszyk W, Dong H-J, Liu C. 2013. Epigenetic upregulation of HGF and c-Met drives metastasis in hepatocellular carcinoma. PloS One 8:e63765.

Plotkin SR, Stemmer-Rachamimov AO, Barker FG 2nd, Halpin C, Padera TP, Tyrrell A, Sorensen AG, Jain RK, di Tomaso E. 2009. Hearing improvement after bevacizumab in patients with neurofibromatosis type 2. N Engl J Med 361:358–367.

Plotkin SR, Halpin C, McKenna MJ, Loeffler JS, Batchelor TT, Barker FG, II. 2010. Erlotinib for progressive vestibular schwannoma in neurofibromatosis 2 patients. Otol Neurotol 31: 1135–1143.

Poage GM, Houseman EA, Christensen BC, Butler RA, Avissar-Whiting M, McClean MD, Waterboer T, Pawlita M, Marsit CJ, Kelsey KT. 2011. Global hypomethylation identifies Loci targeted for hypermethylation in head and neck cancer. Clin Cancer Res 17:3579–3589.

Portela A, Esteller M. 2010. Epigenetic modifications and human disease. Nat Biotechnol 28:1057–1068.

Rao X, Evans J, Chae H, Pilrose J, Kim S, Yan P, Huang R-L, Lai H-C, Lin H, Liu Y, Miller D, Rhee J-K, Huang Y-W, Gu F, Gray JW, Huang T-M, Nephew KP. 2013. CpG island shore methylation regulates caveolin-1 expression in breast cancer. Oncogene 32:4519–4528.

Rey JA, Bello MJ, De Campos JM, Kusak ME, Moreno S. 1987. Cytogenetic analysis in human neurinomas. Cancer Genet Cytogenet 28:187–188.

Richter E, Masuda K, Cook C, Ehrich M, Tadese AY, Li H, Owusu A, Srivastava S, Dobi A. 2007. A role for DNA methylation in regulating the growth suppressor PMEPA1 gene in prostate cancer. Epigenetics 2:100–109.

Robinson JT, Thorvaldsdóttir H, Winckler W, Guttman M, Lander ES, Getz G, Mesirov JP. 2011. Integrative genomics viewer. Nat Biotechnol 29:24–26.

Saeed AI, Sharov V, White J, Li J, Liang W, Bhagabati N, Braisted J, Klapa M, Currier T, Thiagarajan M, Sturn A, Snuffin M, Rezantsev A, Popov D, Ryltsov A, Kostukovich E, Borisovsky I, Liu Z, Vinsavich A, Trush V, Quackenbush J. 2003. TM4: A free, open-source system for microarray data management and analysis. Biotechniques 34:374–378.

Saeed AI, Bhagabati NK, Braisted JC, Liang W, Sharov V, Howe EA, Li J, Thiagarajan M, White JA, Quackenbush J. 2006. TM4 microarray software suite. Methods Enzymol 411: 134–193.

Shen J, Wang S, Zhang Y-J, Wu H-C, Kibriya MG, Jasmine F, Ahsan H, Wu DPH, Siegel AB, Remotti H, Santella RM. 2013. Exploring genome-wide DNA methylation profiles altered in hepatocellular carcinoma using Infinium HumanMethylation 450 BeadChips. Epigenetics 8:34–43.

Su J, Wang Y, Xing X, Liu J, Zhang Y. 2014. Genome-wide analysis of DNA methylation in bovine placentas. BMC Genomics 15:12.

Thorvaldsdóttir H, Robinson JT, Mesirov JP. 2013. Integrative Genomics Viewer (IGV): High-performance genomics data visualization and exploration. Brief Bioinform 14:178–192.

Torres-Martin M, Lassaletta L, de Campos JM, Isla A, Gavilan J, Pinto GR, Burbano RR, Latif F, Melendez B, Castresana JS, Rey JA. 2013a. Global profiling in vestibular schwannomas shows critical deregulation of microRNAs and upregulation in those included in chromosomal region 14q32. PloS One 8:e65868.

Torres-Martin M, Lassaletta L, San-Roman-Montero J, De Campos JM, Isla A, Gavilan J, Melendez B, Pinto GR, Burbano RR, Castresana JS, Rey JA. 2013b. Microarray analysis of gene expression in vestibular schwannomas reveals SPP1/MET signaling pathway and androgen receptor deregulation. Int J Oncol 42:848–862.

Tsunedomi R, Iizuka N, Yoshimura K, Iida M, Tsutsui M, Hashimoto N, Kanekiyo S, Sakamoto K, Tamesa T, Oka M. 2013. ABCB6 mRNA and DNA methylation levels serve as useful biomarkers for prediction of early intrahepatic recurrence of hepatitis C virus-related hepatocellular carcinoma. Int J Oncol 42:1551–1559.

Ushkaryov YA, Petrenko AG, Geppert M, Südhof TC. 1992. Neurexins: Synaptic cell surface proteins related to the alpha-latrotoxin receptor and laminin. Science 257:50–56.

Wang D, Yan L, Hu Q, Sucheston LE, Higgins MJ, Ambrosone CB, Johnson CS, Smiraglia DJ, Liu S. 2012. IMA: An R package for high-throughput analysis of Illumina's 450K Infinium methylation data. Bioinformatics 28:729–730.

Wu D, Terrian DM. 2002. Regulation of caveolin-1 expression and secretion by a protein kinase cepsilon signaling pathway in human prostate cancer cells. J Biol Chem 277:40449–40455.

Xu G, Zhang Y, Wei J, Jia W, Ge Z, Zhang Z, Liu X. 2013. MicroRNA-21 promotes hepatocellular carcinoma HepG2 cell proliferation through repression of mitogen-activated protein kinase-kinase 3. BMC Cancer 13:469.

Yi C, Troutman S, Fera D, Stemmer-Rachamimov A, Avila JL, Christian N, Persson NL, Shimono A, Speicher DW, Marmorstein R, Holmgren L, Kissil JL. 2011. A tight junction-associated Merlin-angiomotin complex mediates Merlin's regulation of mitogenic signaling and tumor suppressive functions. Cancer Cell 19:527–540.

Zhang X, Wu M, Xiao H, Lee M-T, Levin L, Leung Y-K, Ho S-M. 2010. Methylation of a single intronic CpG mediates expression silencing of the PMP24 gene in prostate cancer. Prostate 70:765–776.

Zhang BG, Li JF, Yu BQ, Zhu ZG, Liu BY, Yan M. 2012. microRNA-21 promotes tumor proliferation and invasion in gastric cancer by targeting PTEN. Oncol Rep 27:1019–1026.